

**The novel bis-1,2,4-triazine MIPS-0004373 demonstrates rapid and potent activity
against all blood stages of the malaria parasite**

Running Title: Activity profiling of triazine antimalarial

Katherine M. Ellis^a, Leonardo Lucantoni^b, Marina Chavchich^c, Matthew Abraham^d, Amanda
De Paoli^a, Madeline R. Luth^d, Anne-Marie Zeeman^c, Michael J. Delves^{f*}, Fernando Sánchez-
Román Terán^f, Ursula Straschil^f, Jake Baum^f, Clemens HM. Kocken^e, Stuart A. Ralph^g,
Elizabeth A. Winzeler^d, Vicky M. Avery^b, Michael D. Edstein^c, Jonathan B. Baell^{h#}, Darren
J. Creek^{a#}

^{a.} Drug Delivery Disposition and Dynamics, Monash Institute of Pharmaceutical
Sciences, Monash University, Parkville, VIC 3052, Australia

^{b.} Discovery Biology, Griffith University, Nathan, QLD 4111, Australia

^{c.} The Department of Drug Evaluation, Australian Defence Force Malaria and Infectious
Disease Institute, Brisbane, QLD 4052, Australia

^{d.} School of Medicine, University of California, San Diego, La Jolla, CA, 92093, USA

^{e.} Department of Parasitology, Biomedical Primate Research Centre, Rijswijk,
Netherlands

^{f.} Department of Life Sciences, Imperial College London, Sir Alexander Fleming
Building, Exhibition Road, South Kensington, London, SW7 2AZ, UK

^{g.} Department of Biochemistry and Molecular Biology, Bio21 Molecular Science and
Biotechnology Institute, The University of Melbourne, Parkville, VIC 3052, Australia

^{h.} Medicinal Chemistry, Monash Institute of Pharmaceutical Sciences, Monash
University, Parkville, VIC 3052, Australia

26

27

28 # Address correspondence to Darren Creek, darren.creek@monash.edu or Jonathan Baell,

29 jonathan.baell@monash.edu

30

31 *Present address: Michael J. Delves, London School of Hygiene and Tropical Medicine,

32 London, UK; Fernando Sánchez-Román Terán, Kings College London, London, UK.

33

34 **Keywords:** Malaria, Antimalarial, Triazine, Plasmodium

35

36 **ABSTRACT**

37 Novel bis-1,2,4-triazine compounds with potent *in vitro* activity against *Plasmodium*
38 *falciparum* parasites were recently identified. The bis-1,2,4-triazines represent a unique
39 antimalarial pharmacophore, and are proposed to act by a novel, but as-yet-unknown
40 mechanism of action. This study investigated the activity of the bis-1,2,4-triazine, MIPS-
41 0004373, across the mammalian lifecycle stages of the parasite, and profiled the kinetics of
42 activity against blood and transmission-stage parasites *in vitro* and *in vivo*. MIPS-0004373
43 demonstrated rapid and potent activity against *P. falciparum*, with excellent *in vitro* activity
44 against all asexual blood stages. Prolonged *in vitro* drug exposure failed to generate stable
45 resistance *de novo*, suggesting a low propensity for the emergence of resistance. Excellent
46 activity was observed against sexually-committed ring stage parasites, but activity against
47 mature gametocytes was limited to inhibiting male gametogenesis. Assessment of liver stage
48 activity demonstrated good activity in an *in vitro* *P. berghei* model, but no activity against
49 *P. cynomolgi* hypnozoites or liver schizonts. The bis-1,2,4-triazine, MIPS-0004373,
50 efficiently cleared an established *P. berghei* infection *in vivo*, with efficacy similar to
51 artesunate and chloroquine, and a recrudescence profile comparable to chloroquine. This
52 study demonstrates the suitability of bis-1,2,4-triazines for further development towards a
53 novel treatment for acute malaria.

54

55

56

57 INTRODUCTION

58 Malaria is a parasitic disease caused by infection of red blood cells with the *Plasmodium*
59 parasite. More than 40% of the world's population live in malaria endemic areas and each
60 year there are over 200 million reported cases of malaria. Over 400,000 of these cases result
61 in death, placing malaria as one of the most significant human parasitic diseases (1).
62 Artemisinin-based combination therapies (ACTs) are currently the first line treatments for
63 malaria. Whilst these drug combinations initially displayed a high level of efficacy (2), there
64 have been increasing reports of ACT resistance in South-East Asia over the last decade (3).
65 Since very few novel antimalarial compounds have reached clinical approval in recent times,
66 the increase in parasite resistance to current first line treatments highlights an urgent need for
67 the discovery of new antimalarial medicines (4).

68 The successful development of a new antimalarial will require the drug to demonstrate
69 excellent efficacy, minimal toxicity, low cost, and a lack of cross resistance to existing drugs
70 (5). Furthermore, a recent shift in focus from malaria control to total eradication highlights
71 the necessity for alternative antimalarials with specific activity profiles. New drugs for the
72 treatment of clinical symptoms of blood-stage malaria infection, relapsing malaria, severe
73 malaria or mass drug administration for treatment and transmission blocking are required.
74 Strategies for chemoprevention in endemic areas or chemoprotection for migratory
75 populations as well as outbreak prevention are required. To facilitate the efficient
76 development of drug candidates, the Medicines for Malaria Venture (MMV) have outlined
77 desired target candidate profiles (TCPs) for new antimalarials (Table 1) (4).

78 These target candidate profiles provide guidance regarding the assessment of drug
79 efficacy, pharmacokinetics and toxicity before a compound is progressed towards clinical
80 trials. Ideal requirements of novel antimalarials include potent and rapid clearance of blood
81 stage parasites, suitability as a component of a combination therapy, pharmacokinetics that

82 provide therapeutic blood concentrations for an extended period after a single oral dose, a
83 low toxicity profile, absence of detrimental drug-drug interactions with relapse prevention or
84 transmission blocking molecules, and minimal risk of developing resistance. In addition,
85 activity against other stages of the parasite lifecycle would be an attractive feature to provide
86 the opportunity for prophylactic or transmission-blocking activity.

87 The bis-1,2,4-triazines represent a new class of antimalarial compounds with potent
88 activity against *P. falciparum* that were identified by screening of chemical libraries (6).
89 These compounds, based on a bis-1,2,4-triazine dimer core structure, are currently
90 undergoing optimization by iterative rounds of medicinal chemistry and *in vitro* testing in
91 order to improve potency, selectivity and metabolic stability. A lead triazine dimer MIPS-
92 0004373 (**Fig. 1**) was shown to be highly active *in vitro* against *P. falciparum* with single-
93 digit nanomolar activity and up to several thousand-fold lower toxicity to mammalian cells,
94 thus demonstrating excellent selectivity (6, 7). Furthermore, it was shown to be equipotent
95 against chloroquine and artemisinin resistant laboratory strains of *P. falciparum*, and field
96 isolates of *P. falciparum* and *P. vivax* (8). Pharmacokinetic studies revealed rapid microsomal
97 clearance and low exposure *in vivo*. Nevertheless, excellent *in vivo* activity was observed in
98 the *P. berghei* murine malaria model Peters 4-day test (8), with a 50% effective dose (ED₅₀)
99 of 1.47 mg/kg/day for four days in suppressing the development of blood asexual stages of
100 the rodent malaria. The mechanism of action of the bis-1,2,4-triazines is not known, and their
101 unique structure, compared to other known antimalarials, suggests that these compounds may
102 act via a novel target.

103
104 In this study, MIPS-0004373 was profiled to determine its *in vitro* activity throughout the
105 parasite lifecycle and *in vivo* radical cure efficacy in the *P. berghei*-murine model. Stage
106 specificity within the asexual *P. falciparum* lifecycle, induction of parasite dormancy,

107 transmission blocking ability, liver stage activity and *in vivo* potency were evaluated. We
108 demonstrated MIPS-0004373 to be active against all blood stages of the *P. falciparum*
109 asexual lifecycle and limited (predominantly early) stages of the sexual lifecycle, with a fast
110 onset of action *in vitro* and excellent *in vivo* activity in the modified Thompson test for the
111 radical cure of *P. berghei*. The bis-1,2,4-triazine compound offers great promise for further
112 optimization towards the development of a new medicine for the treatment of symptomatic
113 malaria with potential for transmission blocking activity.

114

115 RESULTS

116 **MIPS-0004373 is highly active against all blood stages of the asexual lifecycle of**
117 ***P. falciparum*.** The *in vitro* stage specific activity of MIPS-0004373 was determined in each
118 of the three stages of the intra-erythrocytic *P. falciparum* asexual lifecycle using a pulsed-
119 exposure format (9). Synchronized ring (3-6 h postinvasion; P.I.), trophozoite (30-36 h P.I.)
120 or schizont (36-40 h P.I.) stage parasites (3D7) were subjected to 5 h drug pulses, washed to
121 remove the triazine compound, and returned to standard culture conditions for a further 48-72
122 h before determination of growth inhibition utilizing the SYBR Green I assay. MIPS-
123 0004373 exhibited potent activity against all parasite stages throughout the asexual lifecycle
124 of *P. falciparum*, displaying IC₅₀ values below 100 nM (Fig. 2a). The highest potency was
125 observed in trophozoite stage parasites (IC₅₀ = 28 nM), although the difference in IC₅₀ values
126 between rings, trophozoites and schizonts was not significant ($P > 0.05$). This similar level of
127 activity exhibited by MIPS-0004373 across the asexual blood stages differentiates the bis-
128 1,2,4-triazines from the clinically used artemisinin- and quinoline-based antimalarials that
129 exhibit more potent activity against the trophozoite and schizont stages (10).

130 The potent activity of MIPS-0004373 against trophozoites exposed to a 5 h drug pulse
131 (IC₅₀ = 28 nM) compared favorably to chloroquine (IC₅₀ = 165 nM) (Fig. 2b), despite similar

132 activity reported from a standard 72 h assay (6). This suggests a rapid onset of action, which
133 was confirmed by the observation of substantial activity after only 1 h of bis-1,2,4-triazine
134 exposure ($IC_{50} = 170$ nM) (Fig. 2b).

135

136 **The bis-1,2,4-triazine inhibits progression from ring to trophozoite stage.** The activity of
137 MIPS-0004373 across all stages of the asexual lifecycle and the rapid onset of action
138 prompted the microscopic assessment of parasite growth over the 48 h lifecycle. Tightly
139 synchronized ring stage *P. falciparum* (3D7; 3 h P.I.) were subjected to a 5 h drug pulse at
140 120 nM (equivalent to twice the IC_{50} of 5 h drug pulse against ring stage parasites), drug was
141 washed out and growth assessed via thin cultured film microscopy at regular time points
142 throughout the remainder of the lifecycle. The addition of MIPS-0004373 had no immediate
143 effect on the size or morphology of ring stage parasites when compared to the DMSO vehicle
144 control (Fig. S1). Differences between treated and untreated parasites only began to appear as
145 the parasites transitioned into the trophozoite stage. At 16-18 h post addition of MIPS-
146 0004373 (19-21 h P.I.), the triazine-treated parasites demonstrated a condensed morphology.
147 While untreated parasites continued to progress through their asexual lifecycle, drug treated
148 parasites showed no further progression.

149

150 **High bis-1,2,4-triazine concentrations arrest ring stage development *in vitro*.** The young
151 ring stage (>95% ~0-5 h P.I.) parasite cultures of the *P. falciparum* W2 laboratory line
152 (parasitemia 0.75- 1.2%) were exposed to either high concentrations of MIPS-0004373 (1200
153 nM or 150x IC_{90}) or dihydroartemisinin (DHA) (700 nM) for 6 h. The same DHA
154 concentration and exposure time have been used in the previously published ring stage
155 survival assay (RSA) (11, 12). The *P. falciparum* W2 line is artemisinin-sensitive and fast

156 growing with parasites completing the asexual cycle within 36-40 h (13) and our observation,
157 as opposed to 48 h cycle for *P. falciparum* *in vivo* or freshly adapted to cultured field isolates.

158 Parasite morphology and recovery after exposure to MIPS-0004373 was evaluated
159 using cultured film microscopy and flow cytometric analysis, using either SYBR Green or
160 Rhodamine 123 dyes, and compared to those after exposure to dihydroartemisinin (DHA)
161 (700 nM) as the reference compound (14). Exposure to MIPS-0004373 arrested progression
162 of rings in a manner similar to what has been previously observed after exposure to DHA
163 (12). Microscopic examination of MIPS-0004373- and DHA-treated cultures revealed similar
164 parasite morphology, with the majority of rings appearing pyknotic with condensed nuclei in
165 the absence of cytoplasm (Fig. S2). Twenty-four hours after the start of the experiment, a
166 small number of parasites demonstrated a morphology consistent with the dormant rings
167 defined by Tucker et al. (15), accounting for $2.5 \pm 0.7\%$ for MIPS-0004373 and $4.0 \pm 0.0\%$
168 for DHA of the total number of ring stage parasites present on the slide. The first growing
169 trophozoites in DHA- and MIPS-000437-treated cultures were detected by cultured film
170 microscopy at 72 h after starting the experiments.

171 In addition to cultured film microscopy analysis, the growth of parasites in untreated
172 controls and cultures exposed to DHA or MIPS-0004373 was followed using flow cytometric
173 analysis of SYBR-Green and Rhodamine 123-stained parasites, with the results of one
174 representative experiment shown in Fig. 3 and Figs. S3 and S4). Twenty-four hours after the
175 start of the experiment the live parasites (Rhodamine 123 stained) in DHA- and MIPS-
176 0004373-treated cultures declined to $0.03 \pm 0.01\%$ and $0.11 \pm 0.01\%$, respectively (Fig. 3)
177 compared to $0.95\% \pm 0.00\%$ in untreated control cultures. Note that the flow cytometric
178 analysis of SYBR-Green stained parasites revealed a significant fraction of MIPS-0004373-
179 treated rings “shifted” to the left in comparison to that in DHA-treated rings, indicative of a

180 greater decrease in fluorescence of SYBR-Green (DNA-binding dye) stained rings,
181 presumably, resulting from DNA degradation (Fig. S3).

182 The parasitemia in treated cultures remained low at 48 h at a value of $0.04\% \pm 0.01\%$
183 for both DHA- and MIPS-0004373-treated cultures. Note that by 48 h parasitemia in the W2
184 line fast growing control cultures reached 7.1%, as judged by microscopy and Sybr-Green,
185 including 1.5% of infected RBC harboring trophozoite stage parasites (Fig S3), thus
186 confirming progression through the 2nd asexual cycle. Note that the “live” parasite numbers
187 were lower, presumably, because of stress on parasites caused by high parasitemia. By 72 h,
188 the W2 line control cultures “crashed”, which resulted in a further reduction in live parasites
189 detected by Rhodamine 123-staining (Fig. S4). A small increase in “live” parasites was
190 detected in cultures exposed to the drugs at 72 h: $0.10 \pm 0.01\%$ and $0.07 \pm 0.00\%$ in DHA-
191 and MIPS-0004373-treated cultures, respectively. During the 168 h of follow-up, more
192 growing parasites were observed in both drug treated cultures, however, the recovery of
193 MIPS-0004373-treated cultures was delayed by at least 24 h in comparison with the DHA-
194 treated cultures (Fig. 3).

195 Treatment of the W2 line cultures with D-sorbitol at 32 h after the start of the
196 experiment, when the majority of W2 control parasites were at late trophozoite and early
197 schizont stage, was used to ascertain if the observed recovery was due to dormant parasites
198 resuming growth or those, which did not become dormant and continued to grow despite
199 DHA or MIPS-0004373 treatment. The application of D-sorbitol in this study was similar to
200 the removal of growing parasites by passaging through magnetic columns (12). The delay in
201 recovery of parasites in cultures exposed to DHA and MIPS-0004373 and subsequently
202 treated with D-Sorbitol, in comparison to those that were not treated, suggest that there were
203 some parasites that were not killed or arrested and continued to grow after drug exposure. In
204 parasite cultures that were treated with D-sorbitol, parasite recovery was delayed by 24 h in

205 DHA-treated cultures (from 72 to 96 h) and by 48 h in MIPS-0004373-treated cultures, from
206 72 to 120 h (Fig 3).

207

208

209 **Attempts to generate bis-1,2,4-triazine resistance *in vitro* were unsuccessful.** Compounds
210 that rapidly generate resistance-conferring mutations in *Plasmodium* are not ideal clinical
211 candidates. Determining the onset of resistance, and potential resistance mechanisms, are
212 important considerations in drug development. Four independent attempts were made to
213 generate resistance to the bis-1,2,4-triazine compound, whereby *P. falciparum* cultures were
214 exposed to MIPS-0004373 over a 3 to 12 month period. The first two attempts subjected 3D7
215 strain parasites to low levels (1x IC₅₀) of MIPS-0004373 (5 nM) and the IC₅₀ was monitored
216 weekly. The first experiment resulted in no significant change in IC₅₀ over a four month
217 period, and parasites were unable to tolerate higher bis-1,2,4-triazine concentrations. In the
218 subsequent attempt it appeared that all parasites died within the first month of bis-1,2,4-
219 triazine exposure (5 nM), and no live parasites were recovered after two more months of
220 continuous culture. In the third attempt to generate resistance, a ramp-up method was
221 employed (16) using the chloroquine resistant Dd2 strain. Initially, parasites were subjected
222 to a 2x IC₅₀ concentration of MIPS-0004373 (Dd2 IC₅₀: 9 nM) and monitored daily by
223 Giemsa stained blood films. After three consecutive days of treatment, cultures reached a
224 parasitemia of ~1% (starting parasitemia ~4%), and required four days of compound-free
225 media to repopulate each test flask before the next round of MIPS-0004373 exposure. This
226 cycle continued for 27 days, after which cultures could tolerate a 3x IC₅₀ concentration of
227 MIPS-0004373 as determined by fractional increases in daily parasitemia while under
228 compound pressure. Over a 6 month course of resistance selections, the maximum treatment
229 concentration used was 4x IC₅₀ (occurring five times), which coincided with a significant

230 decrease in parasitemia. Bulk cultures were evaluated for resistance by dose response assays
231 (IC_{50}) every 2-3 weeks. However, no stable change to the IC_{50} of MIPS-0004373 was
232 observed. The fourth attempt used a similar step-wise method, starting with a different Dd2
233 clone and a 1x IC_{50} concentration (IC_{50} : 13 nM), with 10% concentration increments when
234 tolerated (Fig. S5). Again, no significant increase in IC_{50} of MIPS-0004373 was observed for
235 any of the three replicate flasks over the 12 month period, with the IC_{50} values remaining
236 within 30% of the initial clone. The maximum treatment concentration which allowed
237 recovery (after significant parasite killing) was 2.8 x IC_{50} (37 nM), indicating that none of
238 these attempts were successful at generating bis-1,2,4-triazine-resistant parasites.

239 In addition, no substantial increase in IC_{50} was observed when one of the drug
240 selected lines (attempt 4, rep2) was tested in a ring stage survival assay (Fig S5F). In this
241 assay of 0-3 hour post infection rings, an IC_{50} of 240 ± 18 nM was observed for a 6 hour
242 pulse of MIPS-0004373 compared to the parental Dd2 strain 128 ± 23 nM. This average
243 1.89-fold decrease in activity is comparable to that observed for a standard 48 h assay.
244 Furthermore, no obvious difference in maximal killing was observed at high doses, indicating
245 that no unique ring-stage resistance - such as that associated with artemisinins - was observed
246 for MIPS-0004373.

247

248 To detect variants that may have evolved over the treatment period, four clones from each of
249 the three flasks from the third attempt were isolated and sent for whole genome sequencing.
250 While there were no common mutated genes observed across all clones, it was notable that
251 many of the mutations occurred in genes encoding nuclear proteins involved in epigenetic
252 processes, such as the histone-lysine N-methyltransferase SET2 (PF3D7_1322100) (Table 2,
253 Supplementary Dataset 1).

254

255 **MIPS-0004373 displays limited transmission blocking potential with greatest potency**
256 **against male gametocytes.** The activity of MIPS-0004373 against the sexual stages of the
257 *P. falciparum* lifecycle was assessed to determine the transmission-blocking potential of the
258 bis-1,2,4-triazine. The compound was tested for speed of action against gametocytes, stage-
259 specific inhibition of gametocytes and inhibition of female and male gamete formation. The
260 speed of action of bis-1,2,4-triazines against gametocytes at various stages of development
261 was analysed using the luciferase time to kill assay. Ring stage (day 0) and mature stage V
262 (day 12) NF54^{Pfs16} strain gametocytes were incubated with MIPS-0004373 for 6 h (ring
263 stages only), 24 h, 48 h and 72 h (Fig. 4), followed by measurement of luciferase activity as
264 previously described (17, 18). This activity was then confirmed using the imaging-based
265 stage-specificity study, by incubating ring stage (day 0), early stage (day two), late stage (day
266 eight) and mature stage (day 12) gametocytes with the compound for 48 h, followed by
267 imaging of the plates as previously described (19). MIPS-0004373 displayed potent inhibition
268 of sexually-committed ring stage parasites with an IC₅₀ below 22 nM in both the luciferase
269 and imaging assays. This indicates similar potency to that observed for artemisinin and
270 methylene blue, and greater activity than chloroquine against sexually-committed rings (Fig.
271 4a).

272 The bis-1,2,4-triazine showed a fast onset of action, with killing observed after just 24
273 h treatment against both ring stage and mature gametocytes. However, as gametocytogenesis
274 progressed, MIPS-0004373 showed a gradual decrease in activity. This was confirmed by the
275 imaging stage assay where MIPS-0004373 activity was highest up to stage II of
276 gametocytogenesis, with an IC₅₀ of 5.6 nM. The activity then declined as gametocytogenesis
277 progressed, a 9-fold lower IC₅₀ of 49 nM was observed against stage IV gametocytes (Fig.
278 4b). The luciferase assay confirmed the reduced potency of MIPS-0004373 against stage IV
279 parasites (IC₅₀ = 200 nM). Mature stage V gametocytes appeared largely insensitive to the

280 compound with an $IC_{50} > 5 \mu M$ after a 48 h incubation period. When tested in the acridine
281 orange female gamete formation assay (16), the compound did not inhibit the formation of
282 female gametes up to a concentration of 20 μM .

283 The stage-specific activity of MIPS-0004373 was confirmed using the gametocyte high-
284 content imaging assay (20). Here, efficacy against specific stages of intraerythrocytic
285 gametocytes was determined after a 72 h incubation with MIPS-0004373, using puromycin
286 and DMSO as the positive and negative control, respectively. This assay confirmed potent
287 activity against younger gametocytes, with $>80\%$ reduction in stage I-III counts at MIPS-
288 0004373 concentrations above 154 nM (Fig. S6). The broadened concentration response
289 slope in stages IV-V suggest waning sensitivity to mature forms. Interestingly, significant
290 activity was still observed against mature gametocytes (stage V) with an IC_{50} of 255 ± 169
291 nM in this assay; however, a bottom plateau in the dose-response curve was missing, with
292 maximal gametocytocidal effect (100% inhibition) resulting only at 12.5 μM . This remains
293 significantly less potent than the 1 μM threshold that is commonly used to signify
294 gametocytocidal activity.

295 The activity of the bis-1,2,4-triazine on male and female late stage gametocytes was
296 tested using the dual gamete formation assay (21, 22). It has previously been shown that male
297 gametocytes are more susceptible to a wide range of antimalarial compounds compared to
298 female gametocytes (21). Furthermore, the ratio of gametocytes is generally female-biased
299 (~3-5 females : 1 male), meaning non-sex specific assays may miss compounds that
300 specifically inhibit male gametocytes or male gamete formation. MIPS-0004373 showed low
301 micromolar activity in the male exflagellation assay (3.9 μM) and very slight activity against
302 female gametocytes ($>25 \mu M$) (Fig. 5). Complete parasite inhibition was achieved at the
303 highest concentration of 25 μM for male gametocytes, demonstrating weak activity against
304 the male transmission-specific forms of the parasite.

305

306 **Liver stages demonstrate species-specific susceptibility to bis-1,2,4-triazine treatment.**

307 The activity of MIPS-0004373 was also assessed in the *P. berghei* liver stage assay, adapted
308 from Swann *et al.* (20), which is based on the murine *P. berghei* species transfected to
309 express firefly luciferase. This assay allows for the identification of compounds with activity
310 against sporozoite infection of liver cells as well as those that decrease the viability of liver
311 schizonts. MIPS-0004373 demonstrated potent liver stage activity in this assay (IC₅₀ 199 nM,
312 95% CI: 146.5 – 267.2 nM), with 100% parasite inhibition observed at $\geq 5.55 \mu\text{M}$ (Fig. 6A).
313 A counterscreen with uninfected HepG2 cells was simultaneously performed to measure the
314 potential cytotoxicity of MIPS-0004373 on host liver cells, using puromycin (5 μM) and
315 DMSO (0.5%) as positive and negative controls, respectively. Compounds with 10-fold or
316 greater potency against *P. berghei* liver stage development versus uninfected HepG2 cells
317 can be considered to be specific for the parasite. The average IC₅₀ of MIPS-0004373 in
318 HepG2 was $4.27 \pm 0.099 \mu\text{M}$ (Fig. 6A), suggesting the potent activity against *P. berghei*
319 exoerythrocytic forms is not a function of host cell toxicity.

320 To further investigate liver-stage activity, the *in vitro* *P. cynomolgi* liver stage culture
321 platform (21) was utilized to determine the activity of MIPS-0004373 in a primate malaria
322 model, closely related to *P. vivax*. *P. cynomolgi* is one of the few parasite species that
323 produces hypnozoites, analogous to *P. vivax*. Previous work has found that two populations
324 of parasites could be identified from primate livers infected with *P. cynomolgi*, small forms
325 that resemble hypnozoites and large forms that resemble developing liver stage schizonts
326 (21). MIPS-0004373 showed no activity against either *P. cynomolgi* small or large liver stage
327 forms, even at the highest tested concentration of 10 μM (Fig. 6C).

328 The *in vitro* antimalarial activity profile of MIPS-0004373 that was generated in this
329 study covers various stages of the complex *P. falciparum* lifecycle. This compound

330 represents an exciting new antimalarial series with potency in all asexual blood stage
331 parasites (Table 3i) and a potential to evaluate future analogues for liver stage and
332 transmission blocking activity (Table 3ii).

333

334

335 **MIPS-0004373 effectively clears *P. berghei* infection *in vivo*.** The *in vivo* efficacy of MIPS-
336 0004373 was evaluated in the modified Thompson test (25) over a dose range of 2 to 64
337 mg/kg/day for 3 days against an established murine infection of *P. berghei*. The bis-1,2,4-
338 triazine was well tolerated in mice up to the targeted dose of 64 mg/kg/day for 3 days with no
339 observed physical adverse events such as loss of mobility, poor posture and ruffled fur coat.
340 MIPS-0004373 cleared a mean starting *P. berghei* parasitemia of 2.14% (range: 1.02% to
341 3.26% for the three groups of mice treated with 64 mg/kg/day of the bis-1,2,4-triazine) in
342 about 3 days, which was similar to the speed of action of chloroquine but slightly slower than
343 that of artesunate given the same dose of 64 mg/kg/day for 3 days (Table 4). Lower doses of
344 MIPS-0004373 did not clear the *P. berghei* infections. Daily monitoring of the mice after
345 parasite clearance revealed recrudescences to occur at about day 5 in animals treated with
346 artesunate. In contrast, mice treated with either MIPS-0004373 or chloroquine recrudescenced
347 about 8 days after commencement of treatment. Of note, one mouse with a parasitemia of
348 1.9% before commencement of treatment with 64 mg/kg/day of MIPS-0004373 was still
349 blood film negative at day 31 of follow-up and was deemed to have been cured of the *P.*
350 *berghei* infection. These findings show that the efficacy of MIPS-0004373 in the modified
351 Thompson test is comparable to chloroquine and provides evidence that MIPS-0004373 has a
352 killing effect similar to both artesunate and chloroquine.

353

354

355

356

357 **DISCUSSION**

358 The management of malaria currently relies heavily on the use of ACTs for the treatment of
359 acute falciparum malaria. Recent reports of resistance to ACTs such as dihydroartemisinin-
360 piperazine (26, 27), have emphasized the need to discover new antimalarial medicines with
361 novel mechanisms of action. Excitingly, some novel antimalarial chemotypes have recently
362 entered clinical trials. However, the drug development process is well known to be plagued
363 by attrition, which combined with the inevitable development of antimicrobial resistance,
364 highlights the need to discover and develop new antimalarial chemotypes. In addition, the
365 push towards an elimination and eradication agenda for malaria has gained momentum in
366 recent years, and these ambitious goals will require a range of antimalarials with activity
367 against different stages of the parasite in order to effectively eliminate the spread of disease.
368 The MMV has outlined a range of target candidate profiles with lists of requirements that are
369 necessary to address these specific needs, as described above (Table 1).

370 *In vitro* activity assays identified MIPS-0004373 to be fast acting and potent against
371 all three studied stages of the parasite asexual lifecycle. Importantly, the excellent potency
372 observed against all asexual stages differentiates the bis-1,2,4-triazines from other currently-
373 used antimalarials, providing a potential alternative to artemisinins and an advantage over the
374 currently used quinoline-based compounds (10). The combined potent activity of MIPS-
375 0004373 against ring stage asexual parasites and early stage gametocytes is distinct from
376 currently approved antimalarials and suggests that bis-1,2,4-triazines act by a different
377 mechanism of action. Attempts to generate robustly resistant parasites in order to study
378 potential mechanisms of action and resistance were unsuccessful, though the identification of
379 multiple mutations in epigenetic genes in the parasite clones exposed to MIPS-0004373 over

380 a 6-month period could provide some general clues to the pathway(s) involved in the triazine
381 parasite-killing mechanism. It is possible that the observed mutations provide additional
382 tolerance to the compound without conferring a true resistance phenotype as detected by
383 standard dose-response methods. Alternative approaches are necessary to fully elucidate the
384 mode of action. Nevertheless, the inability to select for robust resistance against this potent
385 bis-1,2,4-triazine compound (MIPS-0004373) after >2 years of cumulative exposure is a
386 promising attribute for future clinical development and usage (16). It has been shown
387 previously that fast acting compounds have a lesser tendency for developing *de novo*
388 resistance. Sanz *et al.* observed a positive correlation between fast onset of action and the
389 inability to generate resistance (16, 28). This agrees with the results that were observed for
390 MIPS-0004373 in the activity assays. Fast acting compounds have many benefits including
391 rapid clearance of parasites, the ability to alleviate symptoms quickly and as mentioned,
392 limiting the development of resistance (16). It has also been suggested that the nature of the
393 target may be responsible for cases where resistance could not be generated, for example the
394 target gene having mutational flexibility or the possibility that the compound inhibits several
395 targets (16).

396 When tested in the rodent *P. berghei* modified Thompson test for radical cure, MIPS-
397 0004373 was as potent as artesunate and chloroquine in clearing an established infection of
398 *P. berghei* by 72 h after commencing oral treatment with 64 mg/kg/day over 3 days.
399 Recrudescence occurred around 8 days after the commencement of MIPS-0004373 treatment,
400 which is comparable to chloroquine, but demonstrates a killing effect similar to both
401 artesunate and chloroquine. This extended activity of MIPS-0004373 is somewhat surprising
402 given that pharmacokinetic studies have shown that MIPS-0004373 is rapidly cleared *in vivo*
403 (8), and may implicate prolonged exposure of an active metabolite, and/or superior reduction
404 of parasitemia immediately following drug exposure. Interestingly, although the *in vitro* ring

405 stage survival assay revealed the presence of some rings with morphology that may indicate
406 the induction of dormancy, similar to those observed following DHA treatment, it did
407 demonstrate a longer time to recrudescence for MIPS-0004373 compared to DHA, which
408 may suggest more efficient parasite killing by MIPS-0004373 even after a short 6 h period of
409 exposure. Overall, the kinetics of antiparasitic activity *in vitro* and *in vivo*, and the inability to
410 select for resistance *in vitro* (to date), support further development of the bis-1,2,4-triazine
411 series to identify a lead candidate for the treatment of symptomatic malaria (TCP-1).

412 MIPS-0004373 displayed no activity against dormant liver stage, *P. cynomolgi*
413 hypnozoites, and is therefore not suitable for relapse prevention (TCP-3). The *in vitro*
414 infection of rhesus hepatocytes by *P. cynomolgi* sporozoites is considered the gold standard
415 for measuring hypnozoite inhibition. However, the disadvantage of this method is the species
416 difference of parasite and host cells. MIPS-0004373 also showed no activity against hepatic
417 schizonts in the *P. cynomolgi* assay, but revealed an IC_{50} of 199 nM against *P. berghei* liver
418 stages. This may indicate species-specific differences in susceptibility of the liver stage
419 parasites, or may suggest activity against the process of invasion and initial infection of
420 hepatocytes in the *P. berghei* model, but inability to clear established infection in the
421 *P. cynomolgi* model. It would be highly beneficial to discover an attractive TCP-4 molecule
422 that displays activity against hepatic schizonts, or casual liver-stage activity, in order to
423 provide chemoprotection. Whilst the lack of activity against *P. cynomolgi* liver stages
424 indicates that the current series of bis-1,2,4-triazines are not suitable as a TCP-4 molecule,
425 further investigations of the chemoprotective potential of this series are warranted. New
426 assays have been developed recently for the analysis of the liver stages of malaria, such as
427 micropatterned primary human hepatocyte co-cultures (29), and it is anticipated that the next
428 generation of bis-1,2,4-triazines could be tested in these alternative assays to further
429 interrogate the liver-stage activity in different parasite and host cell models.

430 MIPS-0004373 displayed potent activity against sexually-committed ring stage parasites,
431 similar to that observed for artemisinin and methylene blue (**Fig. 4**), and was more active
432 than chloroquine. The bis-1,2,4-triazine demonstrated a fast onset of action against both ring
433 stage and mature gametocytes, with growth inhibition observed after 24 h treatment. The
434 observed onset of action is similar to that of artemisinin and methylene blue, suggesting
435 MIPS-0004373 has activity against sexual stage parasites that is comparable to the current
436 first line treatments. The inhibition of late stage gametocytes is a requirement of TCP-5
437 molecules in order to prevent transmission from the human host to the mosquito vector.
438 Based on this criterion, MIPS-0004373 cannot be classified as a TCP-5 molecule, but the low
439 level of activity suggests that further optimization may lead to the discovery of bis-1,2,4-
440 triazine analogues that adequately target this stage. It has been shown that multiple
441 compounds display far greater activity against male stage V gametocytes compared to female
442 gametocytes (21), and MIPS-0004373 follows this trend. It appears that enhanced activity
443 against mature female gametocytes is needed for the bis-1,2,4-triazines to effectively block
444 transmission (TCP-5).

445 This study has demonstrated the suitability of bis-1,2,4-triazine antimalarials to be
446 further investigated for clearance of asexual blood-stage parasitemia (TCP1). Further
447 advancement of the bis-1,2,4-triazine series will focus on optimization of the
448 pharmacokinetic and toxicity profile, while maintaining the excellent anti-parasitic potency.
449 The stage-specific and sex-specific activity against gametocytes, and the species-specific
450 activity against liver-stage schizonts, should be re-assessed with the next-generation of bis-
451 1,2,4-triazines to determine whether preventative or transmission-blocking activity is
452 feasible with this pharmacophore. It will be important to investigate the mechanism of
453 action by which bis-1,2,4-triazine compounds inhibit *P. falciparum* parasite growth, as the
454 identification of the protein target will allow for structure-based design, and for optimal

455 selection of combination regimens to be developed for future clinical usage.

456 Overall, the bis-1,2,4-triazine compounds have the potential to be further developed for
457 the treatment of uncomplicated malaria. Their fast onset of action against all asexual blood
458 stages, sustained suppression of parasitemia *in vivo* and the inability to easily select for
459 resistance are all attractive properties of these bis-1,2,4-triazine compounds.

460

461 MATERIALS AND METHODS

462 **Culturing and tight synchronization of parasites.** Asexual *P. falciparum* 3D7 parasites
463 were cultured under standard conditions (30) with minor modifications, using RBCs
464 (Australian Red Cross Blood Service) at 2% hematocrit in modified RPMI 1640 medium
465 (10.4 g/L), HEPES (5.94 g/L), hypoxanthine (50 mg/L), NaHCO₃ (2.1 g/L) and Albumax (5
466 g/L) at 37°C under a defined atmosphere (Carbogen: 95% N₂, 4% CO₂, 1% O₂). Parasites
467 were routinely synchronized with 5% (wt/vol) D-sorbitol (31). Synchronization and
468 parasitemia were assessed by light microscopic evaluation of Giemsa-stained thin blood films
469 (>500 parasites counted per slide) and the hematocrit determined by counting cells with a
470 Brightline counting chamber hemocytometer (LW scientific).

471 To generate tightly synchronized 3D7 parasites (32), multiple rounds of sorbitol
472 treatments were performed. Cultures were tightly synchronized to a 2- to 3-h window with
473 two sorbitol treatments performed within 14- to 16-h of each other. When mature schizonts
474 began to burst and the ring:schizont ratio was greater than 2:1 a third sorbitol treatment was
475 performed.

476

477 **48 h growth inhibition assay using SYBR Green I.** The antimalarial activity of the bis-
478 1,2,4-triazine compound was determined using a standard drug sensitivity assay (33) by
479 exposing parasites to a drug dilution series (concentrations ranging from 0.25 nM to 200 nM)

480 for 48 h in a 96-well plate format. Briefly, stock solutions of the test compounds prepared in
481 DMSO (1 mM) were first diluted with complete RPMI medium and then serially diluted with
482 medium in a flat-bottomed 96-well plate to achieve a final volume of 50 μ L in each well. An
483 equal volume of parasites was then added to each well to achieve a final parasitemia of 0.5-
484 1% and hematocrit of 2% in 100 μ L of culture medium. Samples maintained under lethal
485 MIPS-0004373 drug pressure (>200 nM) for 48 h acted as the control for 100% parasite
486 killing and infected RBCs incubated without drug acted as the control for 100% parasite
487 growth. Parasite cultures were incubated for 48 h at 37°C under an atmosphere of 1% O₂, 5%
488 CO₂ and 94% N₂.

489 After the 48 h incubation period, parasite drug susceptibility was assessed by the SYBR
490 green assay, as previously described (33). Briefly, the culture medium in each well was
491 refreshed and 100 μ L of lysis buffer containing 0.1 μ L/mL of SYBR Green I was added. The
492 contents of the well were mixed until no RBC sediment remained and the plates were
493 incubated for 1 h in the dark at room temperature. Fluorescence was then measured on an
494 EnSpire Plate Reader (Perkin Elmer) with excitation and emission wavelengths of 485 nm
495 and 530 nm, respectively, and a gain setting of 50 (33, 34). Data analysis was performed
496 using GraphPad Prism (San Diego, CA) software by plotting the fluorescence values against
497 the logarithm of the drug concentration and normalizing by the mean fluorescence intensities
498 for the 100% growth and killing control wells. Curve fitting was performed using the
499 sigmoidal 4 parameter logistic regression (4PL) function to determine the drug concentration
500 that produced 50% growth inhibition (IC₅₀) relative to the drug-free control wells.
501 Experiments were performed with triplicate technical replicates in at least two independent
502 experiments.

503

504 ***In vitro* stage-specificity assays for asexual blood stage *P. falciparum*.** The drug pulse
505 parasite viability assay method was adapted from a previously described method (9). Drug
506 stocks were prepared in fresh RPMI medium and serially diluted with complete RPMI
507 medium in round bottom 96 well microtiter plates. Cultures were adjusted to achieve 1-2%
508 and final hematocrit of iRBCs and uRBCs adjusted to 0.2%. Plates were then incubated for 1
509 h or 5 h at 37 °C under an atmosphere of 1% O₂, 5% CO₂ and 94% N₂. Following the 5 h
510 drug incubation period, cultures were washed three times with 200 µL of complete medium.
511 Cultures were then incubated at 37°C under an atmosphere of 1% O₂, 5% CO₂ and 94% N₂
512 until assessment of parasitemia (~48 h for trophozoite and schizont stage assays, and slightly
513 longer, ~72 h, for ring stage assays to ensure highly sensitive analysis of mature parasites at
514 the time of assessment). Samples maintained under lethal MIPS-0004373 drug pressure
515 (>200 nM) for 48 h acted as the 100% parasite killing control and iRBCs incubated without
516 drug compound acted as the 100% growth control. After lysis, well contents were transferred
517 to a flat bottom 96 well plate for measurement of fluorescence with SYBR green I as
518 described above.

519

520 **Microscopic assessment of growth.** Synchronized ring stage (3 h P.I.) *P. falciparum* were
521 treated with MIPS-0004373 (120 nM) or vehicle (DMSO) control, and incubated for 5 h at
522 37°C under an atmosphere of 1% O₂, 5% CO₂ and 94% N₂. Following the 5 h drug incubation
523 period, cultures were washed three times with complete medium. Cultures were then
524 incubated at 37°C under an atmosphere of 1% O₂, 5% CO₂ and 94% N₂ until assessment of
525 parasitemia. Growth assessment was performed at 10, 16, 18, 20, 22, 24, 26, and 42 h post
526 drug addition, by Giemsa staining and light microscopy.

527

528 **Ring stage survival assay and dormancy assessment.** *P. falciparum* W2 parasites were
529 maintained as described above and routinely synchronized with D-sorbitol. For the dormancy
530 experiments, an additional synchronization with heparin was carried out prior to the
531 experiment (35). Heparin (Pfizer, Australia) was added to culture (2 U/mL of culture) at late
532 trophozoite to early schizont stage to prevent newly-released merozoites from invading
533 RBCs. When cultures reached mature schizont stage, they were centrifuged at $500 \times g$ for 5
534 min, resuspended in complete medium and incubated at 37°C at 90% N₂, 5% CO₂, 5% O₂ for
535 an additional 3 h. Following incubation, the cultures were treated with D-sorbitol to remove
536 remaining schizonts. This process resulted in highly synchronous cultures, typically >95% of
537 parasites at the early ring stage (≤ 3 h P.I.).

538 Young ring (0-3 h P.I.) parasite cultures (3 mL or 6 mL) at 0.75–1.2% parasitemia and
539 4% hematocrit were exposed to MIPS-0004373 (1200 nM; $\sim 150\times$ IC₉₀ for W2) and to the
540 reference drug DHA (stock prepared to 1 mM in 100% methanol) at 700 nM; for 6 h under
541 normal growth conditions. The concentration of DHA (700 nM) used in the present study was
542 in accord with dormancy studies of the W2 *P. falciparum* strain as previously described by
543 Teuscher *et al.* (12) and Witkowski *et al.* (36). Following incubation, the drugs were removed
544 by three washes with medium, resuspended in the original volume of complete medium and
545 incubated at 37°C under normal growth conditions. Three experiments were performed. In
546 the second and third experiments, parasite cultures were split in halves with one half (3 mL)
547 treated with 5% D-sorbitol for 5 min at 30 h from the beginning of drug exposure and the
548 other half left untreated. The D-sorbitol exposure ensures the removal of those parasites that
549 had not become dormant but continued to grow. After sorbitol treatment, the cultures were
550 plated in triplicates into the 96-well plates and monitored for parasite growth by microscopy
551 and flow cytometry for 7–8 d. For flow cytometry analysis, samples (in triplicates) were
552 stained with either the fluorescent nucleic acid intercalating dye, SYBR Green (Invitrogen,

553 Australia) or the mitochondrial vital dye Rhodamine 123 and then quantified by flow
554 cytometry (FC500; Beckman Coulter, Australia). SYBR Green preferentially binds to
555 parasitic nucleic acids and is a measure of parasitic growth but it does not allow for the
556 distinction between dead and growing parasites. In contrast, the uptake of Rhodamine 123 is
557 dependent on the negative mitochondrial membrane potential and is indicative of parasite
558 viability (37).

559 Ring stage survival assays for MIPS-0004373-selected strain (resistance attempt 4,
560 replicate 2; Fig S5F) and the parent Dd2_{clone2} strain were completed in tandem as described
561 above with minor modifications. Briefly, segmented schizonts were magnet harvested and
562 left to invade fresh uRBCs before treatment with 5% (w/v) D-sorbitol 3 hours later to achieve
563 cultures containing only young (0-3 h P.I) ring stage parasites. Cultures at 1% parasitaemia
564 and 2% hematocrit were exposed to a dilution series of MIPS-0004373 starting at 700 nM for
565 6 h under normal growth conditions. Following incubation, the drug was removed by three
566 washes with medium, resuspended in the original volume of complete medium and incubated
567 at 37°C under normal growth conditions for a further 66 h. After which, the activity (RSA_{0-3h}
568 survival rate (%)) was analyzed using the SYBR Green I assay as described above. Three
569 experiments were performed with two technical replicates.

570

571 **Method for development of resistance.** In the first two attempts, 3D7 strain parasites were
572 continually subjected to low levels (1x IC₅₀) of MIPS-0004373 (5 nM). Parasite cultures were
573 maintained as described above, and the activity (IC₅₀) was monitored weekly (if parasites
574 were present) using the SYBR Green I assay described above. Selections occurred over 91
575 and 125 days. When parasites were growing well under these conditions a separate dish was
576 prepared with drug concentration increased to 10 nM, however, parasites did not survive after
577 three lifecycles in these conditions.

578 In the third and fourth attempts, three independent replicates of a clonal *P. falciparum*
579 Dd2 parent population ($\sim 1 \times 10^9$ parasites per replicate) were subjected to increasing
580 concentrations of MIPS-0004373. Cultures were tracked daily by Giemsa stained blood films,
581 and maintained using similar methods to those outlined for 3D7 above. When parasitemia fell
582 below 1-1.5%, cultures were treated with compound-free media and allowed to recrudescence. In
583 order to measure for resistance in each replicate, MIPS-0004373 was tested in dose response
584 as previously described (38). In the third attempt, the primary exposure started at $2 \times IC_{50}$
585 ($Dd2_{clone1} IC_{50}$: 8.75 ± 2.8 nM) and never exceeded $4 \times IC_{50}$ over 186 days. In the fourth
586 attempt, the primary exposure started at $1 \times IC_{50}$ ($Dd2_{clone2} IC_{50}$: 13 nM) and never exceeded
587 $2.8 \times IC_{50}$ over 365 days. After termination of the selection experiment, four clones were
588 isolated from each of three flasks through limiting dilution and sent for whole genome
589 sequencing.

590

591 **Whole genome sequencing and analysis.** Genomic DNA (gDNA) was obtained from MIPS-
592 0004373 selected parasite samples (four clones isolated from each of three flasks in the third
593 attempt described above) by washing infected RBCs with 0.05% saponin and isolating using
594 the DNeasy Blood and Tissue Kit (Qiagen) following standard protocols. Sequencing
595 libraries were prepared by the UCSD Institute for Genomic Medicine (IGM) Genomics
596 Center using the Nextera XT kit (Cat. No FC-131-1024, Illumina) with 2ng input gDNA and
597 standard dual indexing. Libraries were sequenced on the Illumina HiSeq 2500 (PE100,
598 RapidRun mode) to an average of 49x mean whole genome coverage (Table S1). Raw
599 sequencing data were deposited to the NCBI Sequence Read Archive under accession
600 PRJNA748017.

601 Sequencing reads were aligned to the *P. falciparum* 3D7 reference genome
602 (PlasmoDB v13.0) and pre-processed following a previously described pipeline (39).

603 Mutations were called using GATK HaplotypeCaller, filtered by quality according to GATK
604 recommendations (40, 41), and annotated with SnpEff (42). Finally, mutations that were
605 present in both the compound-exposed clones and the non-exposed Dd2 parent line were
606 removed so that mutations in the final variant calling dataset were only retained if they arose
607 during the course of treatment with MIPS-0004373.

608

609

610 **Luciferase gametocyte assay (time to kill study) and AO female gamete formation assay.**

611 *P. falciparum* 3D7A and NF54^{Pfs16} asexual stages were grown in RPMI 1640 supplemented
612 with 25 mM HEPES, 5% AB human male serum, 2.5 mg/mL Albumax II, and 0.37 mM
613 hypoxanthine. Gametocytes were obtained by standard induction methods, described earlier
614 (43). Gametocytes at various stages of development were exposed to the experimental
615 compound in 384-well luciferase (Optiplate, PerkinElmer) or imaging (CellCarrier,
616 PerkinElmer) microplates as previously described (17-19, 44). Artemisinin, chloroquine,
617 dihydroartemisinin, methylene blue, puromycin, pyronaridine, and/or pyrimethamine were
618 used as reference compounds. Puromycin 5 μ M and 0.4% DMSO were used as positive and
619 negative controls, respectively. A 10 mM stock solution of the compound in 100% DMSO
620 was diluted in water (1:25) and culture (1:10) to a final DMSO concentration of 0.4%.
621 Chloroquine stock solution was prepared in water and diluted as the other compounds. All the
622 compounds were tested in either 16-concentration or 21-concentration full dose-response,
623 using three concentrations per log dose. All sample and control wells contained the same
624 final amounts of solvents. Plates were incubated with compounds at 90% N₂, 5% CO₂, 5%
625 O₂. Readout data were normalized to positive and negative controls to obtain % inhibition
626 data, which were then used to calculate IC₅₀ values, through a 4-parameter logistic curve
627 fitting function in GraphPad Prism.

628 The compound was tested for speed of action against gametocytes at different times
629 of development. Ring stage and mature stage V *P. falciparum* NF54^{Pfs16} gametocytes on day
630 0 and day 12 of gametocytogenesis, respectively, were incubated with compounds for 6 h
631 (ring stages only), 24, 48 and 72 h. After the incubation, the luciferase activity was measured
632 as previously described (17, 18). A 0 h-incubation luciferase artifact test was also carried out
633 on sexually-committed rings to rule out an artifactual direct inhibition of the luciferase
634 enzyme. In addition, the compound was tested for female gamete formation by exposing
635 mature stage V gametocytes on day 12 of gametocytogenesis to the compound for 48 h,
636 followed by staining with acridine orange and activation with xanthurenic acid, as previously
637 described (19). The experiment was carried out in two independent experiments, each
638 consisting of two replicates.

639

640 **Gametocyte high-content imaging assay.** Stage specific gametocytes were generated using
641 previously described methods (20). Briefly, 100 mL asexual blood stage cultures of *P.*
642 *falciparum* NF54 were grown to 7-10% parasitemia following a triple synchronization with
643 5% (w/v) D-sorbitol. To induce gametocyte formation, cultures were given 50% spent media
644 for 24 h, followed by daily fresh complete media changes thereafter. Post induction, media
645 was supplemented with 50 mM N-acetyl glucosamine (NAG) for 9 days to prevent reinvasion
646 of asexual stage parasites. 48 h post induction, magnetically activated cell sorting (MACS)
647 was performed followed by sorbitol synchronization the next day. Cultures were followed by
648 daily blood film to determine quantity and maturation of gametocytes. To perform the dose
649 response assay, 50 nL of test compounds (12.5 to 2.12×10^{-4} μ M) were first pre-spotted into
650 black clear bottom 384-well plates (Greiner) using an acoustic transfer system (ATS)
651 (Biosero). Stage specific gametocyte cultures were diluted to 0.50% gametocytemia using
652 serum-free screening media at 1.25% hematocrit, of which 40 μ L were dispensed per well.

653 NAG was added (50 mM) to screening assays containing gametocyte stages I-IV, but not
654 stage V. Breathable metal lids were used to cover the plates, which were incubated at 37°C
655 for 72 h under low oxygen conditions. A solution of MitoTracker® Red CMXRos (2.5 µM)
656 (Life Technologies) and saponin (0.13% w/v) (ACROS Organics, cat. No 419231000) was
657 prepared in screening media, and 10 µL was added to each plate well post incubation. Plates
658 were reincubated at 37°C for 90 min to allow for complete lysis. Test plates were then sealed
659 with adhesive aluminum lids. Images were acquired using an Operetta high content imaging
660 system (PerkinElmer), and image analysis was handled by the onboard Harmony software.
661 All assays were conducted in biological duplicate. Data were normalized against controls,
662 and nonlinear regression analysis was performed in Prism 7 (GraphPad Software, La Jolla,
663 CA) to determine IC₅₀s (log inhibitor versus normalized response – variable slope).

664
665 **Dual gamete formation assay.** MIPS-0004373 and Gentian Violet (positive control) were
666 plated onto 384 well plates in dose response using a Tecan D300e Digital Dispenser. The
667 *P. falciparum* Dual Gamete Formation Assay was performed as described by Delves *et al.*
668 (22). Briefly, gametocyte cultures of NF54 strain *P. falciparum* parasites were initiated at 1%
669 ring parasitemia and culture medium changed whilst maintaining parasites and medium at
670 37°C at all times. On day 14 after induction, when male stage V gametocytes showed high
671 levels of exflagellation when induced, 50 µL of culture at 12.5 million cells per mL (approx.
672 2-4% gametocytemia) was dispensed into each well of compound-treated plates at 37°C.
673 Gametocytes were incubated with compounds for 48 h before gametogenesis was induced by
674 briefly cooling the plate at 4°C and by the addition of ookinete medium containing
675 xanthurenic acid and a Cy3-conjugated antibody specific for Pfs25. Exflagellation was read
676 20 min after induction by automated brightfield microscopy and exflagellation centres
677 identified using custom automated software. Afterwards, the plate was maintained at 26°C in

678 the dark to allow emerged female gametes to express the surface marker Pfs25. 24 h later,
679 female gametes were detected by automated fluorescence microscopy and quantified by
680 custom automated software. Inhibition of male and female gametogenesis was calculated
681 with reference to positive (12.5 μ M Gentian Violet) and negative (DMSO) controls using the
682 following formula:

$$\begin{aligned} 683 \quad \% \text{ inhibition} &= 100 - (((\text{TEST COMPOUND-POSITIVE CONTROL})/(\text{NEGATIVE} \\ 684 \quad &\text{CONTROL-POSITIVE CONTROL})) \times 100) \end{aligned}$$

685 Compounds were tested in four independent replicates.

686

687 ***P. cynomolgi* liver stage assay.** For each batch of *P. cynomolgi* sporozoites required, one
688 rhesus macaque was infected with blood stage parasites, mosquitoes were fed at the
689 appropriate time point and monitored for infection rate (24). Sporozoites were harvested from
690 *P. cynomolgi* infected mosquitoes, around 16 days after the infected blood meal. *In vitro*
691 infections of primary rhesus hepatocytes with *P. cynomolgi* sporozoites (spz) were performed
692 according to Zeeman *et al.* (24). At day six post infection (P.I.) the assays were fixed and
693 stained with anti *P. cynomolgi*-Hsp 70 rabbit antiserum and a FITC-labeled secondary
694 antibody (Goat-anti-rabbit). Plates were analyzed with the Operetta high content imaging
695 system, differentially counting hypnozoites and developing EEFs, based on parasite size (24).

696

697 ***P. berghei* liver stage assay.** Cell maintenance and liver stage activity was evaluated using
698 methods previously described (23). Briefly, 3×10^3 HepG2-A16-CD81^{EGFP} cells were plated
699 per well (5 μ L) of 1536-well, white, opaque-bottom plates (ref# 789173-F, Greiner Bio-One)
700 in DMEM (Invitrogen, Carlsbad, USA) (supplemented with 10% FCS, 0.29 mg/mL
701 glutamine, 100 units penicillin, and 100 μ g/mL streptomycin). Cells were allowed to adhere

702 for 2-4 h before test compounds were added (50 nL/well) in dose response titrations (50 –
703 2.82×10^{-4} μ M) using a Gen 4 Acoustic Transfer System (Biosero) for an 18 h pre-incubation.
704 Atovaquone (1 μ M) and puromycin (5 μ M) were used as positive controls for infected and
705 cytotoxicity plates, respectively. DMSO (0.5%) was used as the negative control in all plates.
706 The next day, *P. berghei*-ANKA-GFP-Luc-SM_{CON} sporozoites were dissected from infected
707 *Anopheles stephensi* mosquitoes, purchased from the insectary core at New York University.
708 Parasite yields were quantified by phase contrast microscopy, and diluted to 200
709 sporozoites/ μ L in media (supplemented with 5x penicillin and streptomycin to inhibit
710 contamination from mosquito debris). 5 μ L of this solution was dispensed (final well volume
711 10 μ L) into each well of an infected plate from a single tip bottle valve liquid handler (GNF),
712 followed by a 3 min centrifugation (Eppendorf 5810 R) at 330 x *g* and low brake. The
713 addition of hepatocytes and compounds were identical for plates evaluating cytotoxicity
714 (uninfected), with a final 5 μ L of clean media added to each well (final well volume 10 μ L).
715 All plates were incubated at 37°C (5% CO₂) and high relative humidity to mitigate media
716 evaporation from wells.

717 After a 48 h incubation, infected plates were inverted and spun at 150 x *g* for 30 s to
718 remove media. BrightGlo (Promega) was then added (2 μ L) to each well using a MicroFlo
719 liquid handler (BioTek). Immediately after the addition, plates were gently tapped to ensure
720 the reagents made contact with the cells before bioluminescence was read using an EnVision
721 Multilabel plate reader (PerkinElmer). CellTiter-Glo (Promega) was first diluted 1:1 before it
722 could be used to quantify bioluminescence in the cytotoxicity assay. Uninfected plates were
723 inverted and spun as before, prior to dispensing 2 μ L of diluted CellTiter-Glo in each plate
724 well. Plates were gently tapped and left for 10 min before reading with an EnVision
725 Multilabel plate reader.

726 For both infected and uninfected assays, IC_{50} s were calculated by normalizing data to
727 controls before fitting a nonlinear regression model (log inhibitor versus normalized response
728 – variable slope) using Prism 7 (GraphPad Software, La Jolla, CA).

729

730 ***In vivo* efficacy of MIPS-0004373 in the modified Thompson test.** Animal Resources
731 Centre (ARC, Perth, Western Australia) female mice (aged 5-7 weeks old, mean body mass
732 of 28.4 ± 1.9 g) in groups of six were infected with 2×10^6 *P. berghei* ANKA strain-
733 infected RBCs on day 0 (D0). By D+3 P.I., parasitemia was typically about 1-3%. The
734 MIPS-0004373 treated groups were administered two-fold increases in MIPS-0004373 dose
735 (e.g., 2 to 64 mg/kg/day). The reference drugs, artesunate and chloroquine were used to gain
736 an insight into the performance of the modified Thompson test at an oral dose of 64
737 mg/kg/day. MIPS-0004373 and artesunate were prepared in Milli-Q water containing 10%
738 ethanol and 10% Tween 80. Chloroquine was dissolved in Milli-Q water. The drugs were
739 administered via oral gavage on days D+3, D+4 and D+5 post-infection at 24 h intervals.
740 Blood samples for flow cytometry and thin blood films were taken daily for 9-10 days and
741 then twice weekly thereafter until the end of the test on day +31.

742 The degree of infection (i.e., parasitemia) was determined by flow cytometry (FC500;
743 Beckman Coulter) using acridine orange as the nucleic acid stain as described by Hein-
744 Kristensen *et al.* (45) with quality assurance using microscopy. The blood samples for flow
745 cytometry and preparation of thin blood films were collected by clipping the mouse's tail tip
746 with a scalpel blade and milking a drop of blood (about 20 μ L). The thin blood film slides
747 were stained with Giemsa for microscopy analysis. For the assessment of radical cure in the
748 modified Thompson test, recurrence of *P. berghei* infection was tabulated for 31 days, at
749 which time all mice surviving that were blood film negative were deemed cured.

750

751 **Ethical approval.** All rhesus macaques (*Macaca mulatta*) used in this study were captive
752 bred for research purposes and were housed at the BPRC facilities under compliance with the
753 Dutch law on animal experiments, European directive 2010/63/EU and with the ‘Standard for
754 humane care and use of Laboratory Animals by Foreign institutions’ identification number
755 A5539-01, provided by the Department of Health and Human Services of the USA National
756 Institutes of Health (NIH). The BPRC is an AAALAC-certified institute. Prior to the start of
757 monkey experiments, protocols were approved by the local independent ethical committee,
758 according to Dutch law. The procedures used for the *in vivo* efficacy studies in mice were in
759 accordance with the Australian Code of Practice for the Care and Use of Animals for
760 Scientific Purposes. The ethical approval to conduct tolerability and efficacy study of MIPS-
761 0004373 in the *P. berghei*-mouse model using the modified Thompson test was approved by
762 the Defence Animal Ethics Committee, Australian Defence Organisation (approval numbers:
763 3/2014, 03/2015 and 02/2016).

764

765 **ACKNOWLEDGEMENTS**

766 We are grateful to Kerry Rowcliffe for technical support in *in vitro* dormancy assay and
767 thank the Australian Red Cross Blood Service for the provision of human blood, plasma and
768 sera for *in vitro* cultivation of *P. falciparum* lines at Monash University, ADFMIDI and
769 Griffith University. We also thank Donna MacKenzie, Geoff Birrell, Ivor Harris and Stephen
770 McLeod-Robertson for the *in vivo* efficacy testing of MIPS-0004373 in the *P. berghei*-rodent
771 model. The views expressed in this article are those of the authors and do not necessarily
772 reflect those of the Australian Defence Force Joint Health Command or any extant Australian
773 Defence Force policy. Funding support has been provided by the Australian National Health
774 and Medical Research Council (NHMRC) project grant #APP1102147 and fellowships to
775 DJC (#APP1148700) and JBB (#APP1117602). AMZ and CHMK were supported by the

776 Medicines for Malaria Venture (MMV). MRL was supported in part by a Ruth L. Kirschstein
777 Institutional National Research Award from the National Institute for General Medical
778 Sciences (T32 GM008666). We thank Nicole van der Werff and Ivonne Nieuwenhuis for
779 expert help with the *P. cynomolgi* drug assays. Gametocyte time to kill and AO female
780 gamete studies supported by MMV grant to VMA. Gamete formation screening was
781 supported by MMV grant to JB (RD-08-2800), and an Investigator Award from Wellcome to
782 JB (100993/Z/13/Z).

783

784

785 REFERENCES

786

- 787 1. Noor A, Aponte J, Aregawi M, Barrette A, Biondi N, Knox T, Patouillard E, Williams
788 R. 2017. World Malaria Report 2017. WHO, WHO.
- 789 2. Dondorp AM, Yeung S, White L, Nguon C, Day NPJ, Socheat D, von Seidlein L.
790 2010. Artemisinin resistance: current status and scenarios for containment. Nat Rev
791 Micro 8:272-280.
- 792 3. Yeung S, Socheat D, Moorthy V, Mills A. 2009. Artemisinin resistance on the Thai-
793 Cambodian border. Lancet 374:1418 - 1419.
- 794 4. Burrows JN, Duparc S, Gutteridge WE, Hooft van Huijsduijnen R, Kaszubska W,
795 Macintyre F, Mazzuri S, Möhrle JJ, Wells TNC. 2017. New developments in anti-
796 malarial target candidate and product profiles. Malar J 16:26.
- 797 5. Burrows J, Hooft van Huijsduijnen R, Mohrle J, Oeuvray C, Wells T. 2013.
798 Designing the next generation of medicines for malaria control and eradication. Malar
799 J 12:187.

- 800 6. Ban K, Duffy S, Khakham Y, Avery VM, Hughes A, Montagnat O, Katneni K, Ryan
801 E, Baell JB. 2010. 3-Alkylthio-1,2,4-triazine dimers with potent antimalarial activity.
802 Bioorg Med Chem Lett 20:6024-6029.
- 803 7. Priebbenow DL, Mathiew M, Shi D-H, Harjani JR, Beveridge JG, Chavchich M,
804 Edstein MD, Duffy S, Avery VM, Jacobs RT, Brand S, Shackleford DM, Wang W, Zhong L,
805 Lee G, Tay E, Barker H, Crighton E, White KL, Charman SA, De Paoli A, Creek DJ, Baell
806 JB. 2021. Discovery of potent and fast-acting antimalarial bis-1,2,4-triazines. J Med Chem
807 64:4150-4162.
- 808 8. Xue L, Shi DH, Harjani JR, Huang F, Beveridge JG, Dingjan T, Ban K, Diab S, Duffy
809 S, Lucantoni L, Fletcher S, Chiu FCK, Blundell S, Ellis K, Ralph SA, Wirjanata G, Teguh S,
810 Noviyanti R, Chavchich M, Creek D, Price RN, Marfurt J, Charman SA, Cuellar ME,
811 Strasser JM, Dahlin JL, Walters MA, Edstein MD, Avery VM, Baell JB. 2019. 3,3'-
812 Disubstituted 5,5'-bi(1,2,4-triazine) derivatives with potent in vitro and in vivo antimalarial
813 activity. J Med Chem 62:2485-2498.
- 814 9. Yang T, Xie SC, Cao P, Giannangelo C, McCaw J, Creek DJ, Charman SA, Klonis N,
815 Tilley L. 2016. Comparison of the exposure time dependence of the activities of
816 synthetic ozonide antimalarials and dihydroartemisinin against K13 wild-type and
817 mutant *Plasmodium falciparum* strains. Antimicrob Agents Chemother 60:4501-
818 4510.
- 819 10. Klonis N, Xie SC, McCaw JM, Crespo-Ortiz MP, Zaloumis SG, Simpson JA, Tilley
820 L. 2013. Altered temporal response of malaria parasites determines differential
821 sensitivity to artemisinin. Proc Natl Acad Sci 110:5157-5162.
- 822 10. Witkowski B, Khim N, Chim P, Kim S, Ke S, Kloeung N, Chy S, Duong S, Leang R,
823 Ringwald P, Dondorp AM, Tripura R, Benoit-Vical F, Berry A, Gorgette O, Arieu F,
824 Barale J-C, Mercereau-Puijalon O, Menard D. 2013. Reduced artemisinin

- 825 susceptibility of *Plasmodium falciparum* ring stages in western Cambodia.
- 826 Antimicrob Agents Chemother 57:914-923.
- 827 11.12. Teuscher F, Gatton ML, Chen N, Peters J, Kyle DE, Cheng Q. 2010. Artemisinin-
- 828 induced dormancy in *Plasmodium falciparum*: duration, recovery rates, and
- 829 implications in treatment failure. J Infect Dis 202:1362-1368.
- 830 13. Veiga MI, Ferreira PE, Schmidt BA, Ribacke U, Björkman A, Tichopad A, Gil JP.
- 831 2010. Antimalarial exposure delays *Plasmodium falciparum* intra-erythrocytic cycle and
- 832 drives drug transporter genes expression. PLOS ONE 5:e12408.
- 833 14. Peatey CL, Chavchich M, Chen N, Gresty KJ, Gray KA, Gatton ML, Waters NC,
- 834 Cheng Q. 2015. Mitochondrial membrane potential in a small subset of artemisinin-induced
- 835 dormant *Plasmodium falciparum* parasites *in vitro*. J Infect Dis 212:426-34.
- 836 15. Tucker MS, Mutka T, Sparks K, Patel J, Kyle DE. 2012. Phenotypic and genotypic
- 837 analysis of in vitro-selected artemisinin-resistant progeny of *Plasmodium falciparum*.
- 838 Antimicrob Agents Chemother 56:302-314.
- 839 16. Corey VC, Lukens AK, Istvan ES, Lee MCS, Franco V, Magistrado P, Coburn-Flynn
- 840 O, Sakata-Kato T, Fuchs O, Gnädig NF, Goldgof G, Linares M, Gomez-Lorenzo MG,
- 841 De Cózar C, Lafuente-Monasterio MJ, Prats S, Meister S, Tanaseichuk O, Wree M,
- 842 Zhou Y, Willis PA, Gamo F-J, Goldberg DE, Fidock DA, Wirth DF, Winzeler EA.
- 843 2016. A broad analysis of resistance development in the malaria parasite. Nat
- 844 Commun 7:11901.
- 845 17. Lucantoni L, Duffy S, Adjalley SH, Fidock DA, Avery VM. 2013. Identification of
- 846 MMV malaria box inhibitors of *Plasmodium falciparum* early-stage gametocytes,
- 847 using a luciferase-based high-throughput assay. Antimicrob Agents Chemother
- 848 57:6050-62.

- 849 18. Lucantoni L, Fidock DA, Avery VM. 2016. A luciferase-based, high-throughput
850 assay for screening and profiling transmission-blocking compounds against
851 *Plasmodium falciparum* gametocytes. Antimicrob Agents Chemother 60:2097-107.
- 852 19. Lucantoni L, Silvestrini F, Signore M, Siciliano G, Eldering M, Dechering KJ, Avery
853 VM, Alano P. 2015. A simple and predictive phenotypic High Content Imaging assay
854 for *Plasmodium falciparum* mature gametocytes to identify malaria transmission
855 blocking compounds. Sci Rep 5:16414.
- 856 20. Plouffe DM, Wree M, Du AY, Meister S, Li F, Patra K, Lubar A, Okitsu SL, Flannery
857 EL, Kato N, Tanaseichuk O, Comer E, Zhou B, Kuhlen K, Zhou Y, Leroy D,
858 Schreiber SL, Scherer CA, Vinetz J, Winzeler EA. 2016. High-throughput assay and
859 discovery of small molecules that interrupt malaria transmission. Cell Host Microbe
860 19:114-126.
- 861 21. Ruecker A, Mathias DK, Straschil U, Churcher TS, Dinglasan RR, Leroy D, Sinden
862 RE, Delves MJ. 2014. A male and female gametocyte functional viability assay to
863 identify biologically relevant malaria transmission-blocking drugs. Antimicrob
864 Agents Chemother 58:7292-7302.
- 865 22. Delves MJ, Straschil U, Ruecker A, Miguel-Blanco C, Marques S, Dufour AC, Baum
866 J, Sinden RE. 2016. Routine *in vitro* culture of *P. falciparum* gametocytes to evaluate
867 novel transmission-blocking interventions. Nat Protoc 11:1668.
- 868 23. Swann J, Corey V, Scherer CA, Kato N, Comer E, Maetani M, Antonova-Koch Y,
869 Reimer C, Gagaring K, Ibanez M, Plouffe D, Zeeman A-M, Kocken CHM,
870 McNamara CW, Schreiber SL, Campo B, Winzeler EA, Meister S. 2016. High-
871 throughput luciferase-based assay for the discovery of therapeutics that prevent
872 malaria. ACS Infect Dis 2:281-293.

- 873 24. Zeeman A-M, van Amsterdam SM, McNamara CW, Voorberg-van der Wel A,
874 Klooster EJ, van den Berg A, Remarque EJ, Plouffe DM, van Gemert G-J, Luty A,
875 Sauerwein R, Gagaring K, Borboa R, Chen Z, Kuhen K, Glynne RJ, Chatterjee AK,
876 Nagle A, Roland J, Winzeler EA, Leroy D, Campo B, Diagana TT, Yeung BKS,
877 Thomas AW, Kocken CHM. 2014. KAI407, a potent non-8-aminoquinoline
878 compound that kills *Plasmodium cynomolgi* early dormant liver stage parasites *in*
879 *vitro*. Antimicrob Agents Chemother 58:1586-1595.
- 880 25. Ager AL. 1984. Rodent malaria models, p 225-264. In Peters W, Richards WHG (ed),
881 Antimalarial Drugs I: Biological Background, Experimental Methods, and Drug
882 Resistance doi:10.1007/978-3-662-35326-4_8. Springer Berlin Heidelberg, Berlin,
883 Heidelberg.
- 884 26. Saunders DL, Vanachayangkul P, Lon C. 2014. Dihydroartemisinin-piperaquine
885 failure in Cambodia. N Engl J Med 371:484-485.
- 886 27. Thanh NV, Thuy-Nhien N, Tuyen NTK, Tong NT, Nha-Ca NT, Dong LT, Quang
887 HH, Farrar J, Thwaites G, White NJ, Wolbers M, Hien TT. 2017. Rapid decline in the
888 susceptibility of *Plasmodium falciparum* to dihydroartemisinin-piperaquine in the
889 south of Vietnam. Malar J 16:27.
- 890 28. Sanz L, Crespo B, De-Cozar C, Ding X, Llergo J, Burrows J, Garcia-Bustos J, Gamo
891 F. 2012. *P. falciparum in vitro* killing rates allow to discriminate between different
892 antimalarial mode-of-action. PLoS One 7:e30949.
- 893 29. Gural N, Mancio-Silva L, Miller AB, Galstian A, Butty VL, Levine SS, Patrapuvich
894 R, Desai SP, Mikolajczak SA, Kappe SH. 2018. *In vitro* culture, drug sensitivity, and
895 transcriptome of *Plasmodium vivax* hypnozoites. Cell Host Microbe 23:395-406.e4.
- 896 30. Trager W, Jensen JB. 1976. Human malaria parasites in continuous culture. Science
897 193:673-675.

- 898 31. Lambros C, Vanderberg JP. 1979. Synchronization of *Plasmodium falciparum*
899 erythrocytic stages in culture. J Parasitol 65:418-420.
- 900 32. Straimer J, Gnädig NF, Witkowski B, Amaratunga C, Duru V, Ramadani AP,
901 Dacheux M, Khim N, Zhang L, Lam S, Gregory PD, Urnov FD, Mercereau-Puijalon
902 O, Benoit-Vical F, Fairhurst RM, Ménard D, Fidock DA. 2015. K13-propeller
903 mutations confer artemisinin resistance in *Plasmodium falciparum* clinical isolates.
904 Science 347:428-431.
- 905 33. Smilkstein M, Sriwilaijaroen N, Kelly JX, Wilairat P, Riscoe M. 2004. Simple and
906 inexpensive fluorescence-based technique for high-throughput antimalarial drug
907 screening. Antimicrob Agents Chemother 48:1803-1806.
- 908 34. Johnson JD, Dennull RA, Gerena L, Lopez-Sanchez M, Roncal NE, Waters NC.
909 2007. Assessment and continued validation of the malaria SYBR Green I-based
910 fluorescence assay for use in malaria drug screening. Antimicrob Agents Chemother
911 51:1926-1933.
- 912 35. Boyle MJ, Wilson DW, Richards JS, Riglar DT, Tetteh KK, Conway DJ, Ralph SA,
913 Baum J, Beeson JG. 2010. Isolation of viable *Plasmodium falciparum* merozoites to
914 define erythrocyte invasion events and advance vaccine and drug development. Proc
915 Natl Acad Sci Define Erythrocyte Invasion Events and Advance Vaccine and Drug
916 Development. Proceedings of the National Academy of Sciences of the United States
917 of America 107:14378-14383.
- 918 36. Witkowski B, Amaratunga C, Khim N, Sreng S, Chim P, Kim S, Lim P, Mao S, Sopha C,
919 Sam B, Anderson JM, Duong S, Chuor CM, Taylor WRJ, Suon S, Mercereau-Puijalon O,
920 Fairhurst RM, Menard D. 2013. Novel phenotypic assays for the detection of artemisinin-
921 resistant *Plasmodium falciparum* malaria in Cambodia: *in-vitro* and *ex-vivo* drug-response
922 studies. Lancet Infect Dis 13:1043-1049.

- 923 37. Izumo A, Tanabe K, Kato M. 1987. A method for monitoring the viability of malaria
924 parasites (*Plasmodium yoelii*) freed from the host erythrocytes. Trans R Soc Trop
925 Med Hyg 81:264-267.
- 926 38. Plouffe D, Brinker A, McNamara C, Henson K, Kato N, Kuhlen K, Nagle A, Adrián
927 F, Matzen JT, Anderson P, Nam T-G, Gray NS, Chatterjee A, Janes J, Yan SF, Trager
928 R, Caldwell JS, Schultz PG, Zhou Y, Winzeler EA. 2008. *In silico* activity profiling
929 reveals the mechanism of action of antimalarials discovered in a high-throughput
930 screen. Proc Natl Acad Sci 105:9059-9064.
- 931 39. Cowell AN, Istvan ES, Lukens AK, Gomez-Lorenzo MG, Vanaerschot M, Sakata-
932 Kato T, Flannery EL, Magistrado P, Owen E, Abraham M, LaMonte G, Painter HJ, Williams
933 RM, Franco V, Linares M, Arriaga I, Bopp S, Corey VC, Gnädig NF, Coburn-Flynn O,
934 Reimer C, Gupta P, Murithi JM, Moura PA, Fuchs O, Sasaki E, Kim SW, Teng CH, Wang
935 LT, Akidil A, Adjalley S, Willis PA, Siegel D, Tanaseichuk O, Zhong Y, Zhou Y, Llinás M,
936 Otilie S, Gamo FJ, Lee MCS, Goldberg DE, Fidock DA, Wirth DF, Winzeler EA. 2018.
937 Mapping the malaria parasite druggable genome by using *in vitro* evolution and
938 chemogenomics. Science 359:191-199.
- 939 40. McKenna A, Hanna M, Banks E, Sivachenko A, Cibulskis K, Kernysky A, Garimella
940 K, Altshuler D, Gabriel S, Daly M, DePristo MA. 2010. The Genome Analysis Toolkit: a
941 MapReduce framework for analyzing next-generation DNA sequencing data. Genome Res
942 20:1297-303.
- 943 41. Van der Auwera GA, Carneiro MO, Hartl C, Poplin R, Del Angel G, Levy-
944 Moonshine A, Jordan T, Shakir K, Roazen D, Thibault J, Banks E, Garimella KV, Altshuler
945 D, Gabriel S, DePristo MA. 2013. From FastQ data to high confidence variant calls: the
946 Genome Analysis Toolkit best practices pipeline. Curr Protoc Bioinform 43:11.10.1-
947 11.10.33.

- 948 42. Cingolani P, Platts A, Wang le L, Coon M, Nguyen T, Wang L, Land SJ, Lu X,
949 Ruden DM. 2012. A program for annotating and predicting the effects of single nucleotide
950 polymorphisms, SnpEff: SNPs in the genome of *Drosophila melanogaster* strain w1118; iso-
951 2; iso-3. Fly 6:80-92.
- 952 43. Duffy S, Loganathan S, Holleran JP, Avery VM. 2016. Large-scale production of
953 *Plasmodium falciparum* gametocytes for malaria drug discovery. Nat Protoc 11:976.
- 954 44. Duffy S, Avery VM. 2013. Identification of inhibitors of *Plasmodium falciparum*
955 gametocyte development. Malar J 12:408.
- 956 45. Hein-Kristensen L, Wiese L, Kurtzhals JA, Staalsoe T. 2009. In-depth validation of
957 acridine orange staining for flow cytometric parasite and reticulocyte enumeration in
958 an experimental model using *Plasmodium berghei*. Exp Parasitol 123:152-7.
- 959
960
961

962 **Tables:**

963 **TABLE 1.** Summary of MMV target candidate profiles (TCPs) for new antimalarial
964 medicines (4).

Profile	Intended use
TCP-1	Molecules that clear asexual blood-stage parasitemia
TCP-3	Molecules with activity against hypnozoites (mainly <i>P. vivax</i>)
TCP-4	Molecules with activity against hepatic schizonts
TCP-5	Molecules that block transmission (targeting parasite gametocytes)
TCP-6	Molecules that block transmission by targeting the insect vector (endectocides)

965

966

967 **TABLE 2.** Select coding mutations identified in Dd2 parasites exposed to MIPS-0004373 for
968 6 months. The full set of mutations are provided in Supplementary Dataset 1.

Flask	Clone Name	Gene ID	Gene Description	Mutation Type	Amino Acid Change
1	A9	PF3D7_0510100	KH domain-containing protein	Disruptive inframe deletion	Ser2328_Gly2332del
		PF3D7_1471600	conserved <i>Plasmodium</i> protein, unknown function	Missense	Asp987Tyr
	B3	PF3D7_1322100	histone-lysine N-methyltransferase SET2	Nonsense	Leu884*
	D1	PF3D7_0609200	citrate synthase-like protein	Missense	Asn39Tyr
		PF3D7_1322100	histone-lysine N-methyltransferase SET2	Nonsense	Leu884*
	H8	No coding mutations of interest			
2	D3	PF3D7_1462400	conserved <i>Plasmodium</i> protein, unknown function	Nonsense	Tyr2603*
	D12	PF3D7_1008100	PHD finger protein PHD1	Missense	His1762Tyr
		PF3D7_1456500	STAG domain-containing protein	Missense	Thr66Ala
		PF3D7_1462400	conserved <i>Plasmodium</i> protein, unknown function	Nonsense	Tyr2603*
	F8	No coding mutations of interest			
	H1	PF3D7_1459200	WD repeat-containing protein	Frameshift	Val359fs
3	B11	PF3D7_1322100	histone-lysine N-	Nonsense	Leu884*

			methyltransferase SET2		
	C9	PF3D7_1205500	zinc finger protein	Missense	Trp678Leu
	F1	No coding variants of interest			
	H6	PF3D7_1322100	histone-lysine N-methyltransferase SET2	Nonsense	Leu884*

969

970 **TABLE 3.** Summary of MIPS-0004373 activity across the complex *P. falciparum* lifecycle.971 **i.** IC₅₀ data of asexual staged parasites from liver and blood cycles **ii.** IC₅₀ data of sexual

972 stages.

3i	Summary of MIPS-0004373 activity of asexual stage <i>P. cynomolgi</i> , <i>P. berghei</i> or <i>P. falciparum</i> (nM)					Fig#
	Liver stage	Ring	Trophozoite	Schizont	Asynchronous stages	
<i>P. cynomolgi</i> (hypnozoite inhibition)	>10 000					6A
<i>P. berghei</i> 48 h IC ₅₀ survival assay	199 (46.5-267.2)*					6B
<i>P. falciparum</i> 3D7 1 h pulse IC ₅₀ survival assay			171 ± 62			2B
<i>P. falciparum</i> 3D7 5 h pulse IC ₅₀ survival assay		61 ± 29	28 ± 8, 32 ± 11	56 ± 3		2A, 2B
<i>P. falciparum</i> 3D7 48 h IC ₅₀ survival assay			4 ± 1			2B
<i>P. falciparum</i> 3D7 72 h IC ₅₀ survival assay					8 ± 4	Ref (6)

973 Values show the mean ± SD of at least three biological replicates with at least two technical

974 repeats. *95% confidence interval.

3ii	Summary of MIPS-0004373 activity of sexual stage <i>P. falciparum</i> (nM)						Fig #
	Committed ring	Stage IV gametocyte	Mature stage V gametocyte	Male	Female		
NF54 24 h time to kill assay	3 ± 1		>1000				4A
NF54 48 h time to kill assay	8 ± 3		4514 ± 1635				4A

NF54 72 h time to kill assay	22 ± 5			1997 ± 1335			4A
72 h NF54 high content imaging assay	5 ± 0.1	6 ± 1	49 ± 15	255 ± 169			4B
Dual gamete formation assay					3903 ± 184*	> 25 000*	5
AO female gamete assay						>20 000	

975 Data shows the means ± SEM of two biological replicates with two technical replicates.

976 *Mean ± SD of one biological experiment with four replicates.

977

978 **TABLE 4.** *In vivo* efficacy of MIPS-0004373, artesunate and chloroquine against established979 *P. berghei* infection in the modified Thompson test.

	Dose 64 mg/kg/day x 3	Experiment 1.	Experiment 2.	Experiment 3.
Starting parasitemia* (%) for treatment at D0 (mean: range)		1.68 (0.54-3.26)	1.68 (1.43-2.13)	1.65 (1.02-2.23)
Day of parasite clearance after starting treatment	MIPS-0004373	D+3	D+4	D+2
	Artesunate	D+3	D+2	D+2
	Chloroquine	D+3	D+3	D+3
Day of recrudescence after starting treatment	MIPS-0004373	D+8	D+7	D+8
	Artesunate	D+5	D+5	D+4
	Chloroquine	D+8	D+8	D+8

980 *Mean (range) parasitemia values based on flow cytometry for the drug treated and vehicle

981 control groups of mice. N = 6 mice per group.

982

983

984

985 **Figure Legends**

986

987 **Figure 1:** The representative bis-1,2,4-triazine, MIPS-0004373

988

989 **Figure 2:** *In vitro* assessment of stage-specificity and rate of action of MIPS-0004373 against
990 the 3D7 strain of *P. falciparum*. **A.** Asexual blood stage IC₅₀ values for MIPS-0004373
991 against early ring stages (3-6 h P.I.), trophozoites (30-36 h P.I.) and schizonts (36-40 h P.I.)
992 after a 5 h pulse. **B.** IC₅₀ values for MIPS-0004373 (black bars) and chloroquine (grey bars)
993 after 1, 5 and 48 h drug pulses against *P. falciparum* trophozoites (30-36 h P.I.). Graphs show
994 the mean \pm SD, n = 5.

995
996 **Figure 3:** Live parasite dynamics following 6 h exposure to MIPS-0004373 or DHA. The
997 live *P. falciparum* W2 parasites were detected by staining with Rhodamine 123. At 32 h after
998 the commencement of the experiment, the cultures were split and one half was treated with
999 5% sorbitol (designated as W2 Control/Sorb, MIPS-0004373/Sorb and DHA/Sorb, whereas
1000 the other half was left untreated (designated as W2 Control, MIPS-0004373, DHA). Means \pm
1001 SD based on two independent experiments, each consisting of triplicate replicates.

1002
1003 **Figure 4:** Activity and speed of action of MIPS-0004373 against gametocytes. **A.** Sexually-
1004 committed rings (SCR) and mature stage gametocytes (MSG) were exposed to the compound
1005 for 24, 48 or 72 h and gametocyte inhibition was analysed by luciferase activity. IC₅₀ curves
1006 for MIPS-0004373 (red), methylene blue (blue), puromycin (green), chloroquine (yellow)
1007 and artemisinin (pink). Puromycin was included as the positive control. Two independent
1008 experiments, each consisting of two replicates. **B.** The bis-1,2,4-triazine potently inhibits
1009 sexually-committed rings, although it has low activity on mature gametocytes. IC₅₀ curves for
1010 sexually-committed rings (green), day two early stage gametocytes (blue), day eight late
1011 stage gametocytes (black), and day 12 MSG (red). Data shows the means \pm SEM of two
1012 biological replicates with two technical replicates.

1013

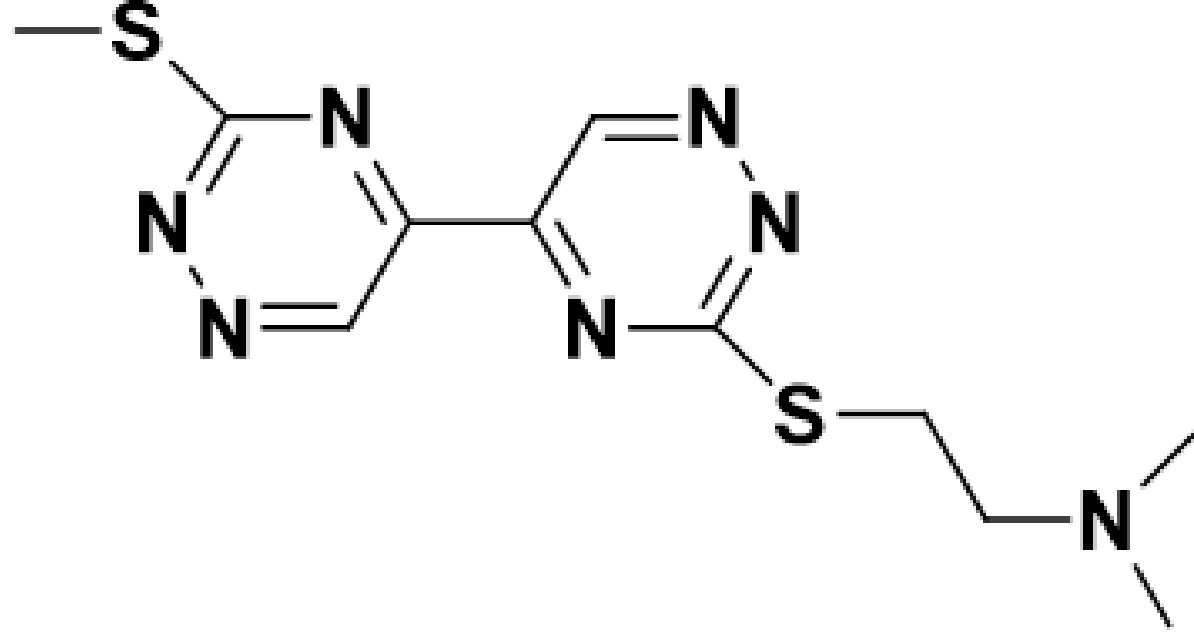
1014 **Figure 5:** Bis-1,2,4-triazine activity in late stage male and female gametocytes. IC₅₀ curves
1015 for **A.** the control compound, Gentian Violet, and **B.** MIPS-0004373 in male gametocytes
1016 (blue) and female gametocytes (red). Data shows the means \pm SD of one biological
1017 experiment with four replicates.

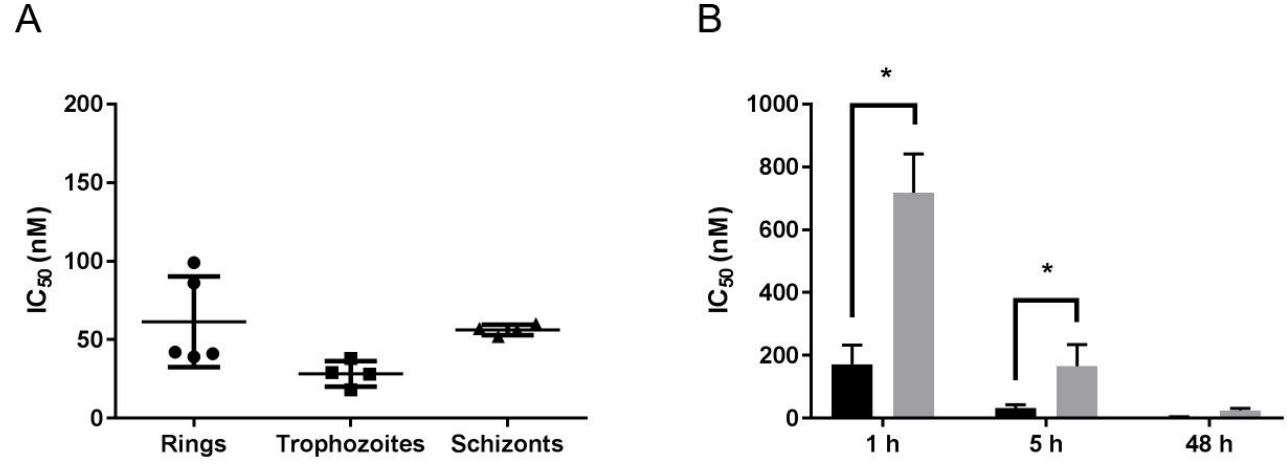
1018

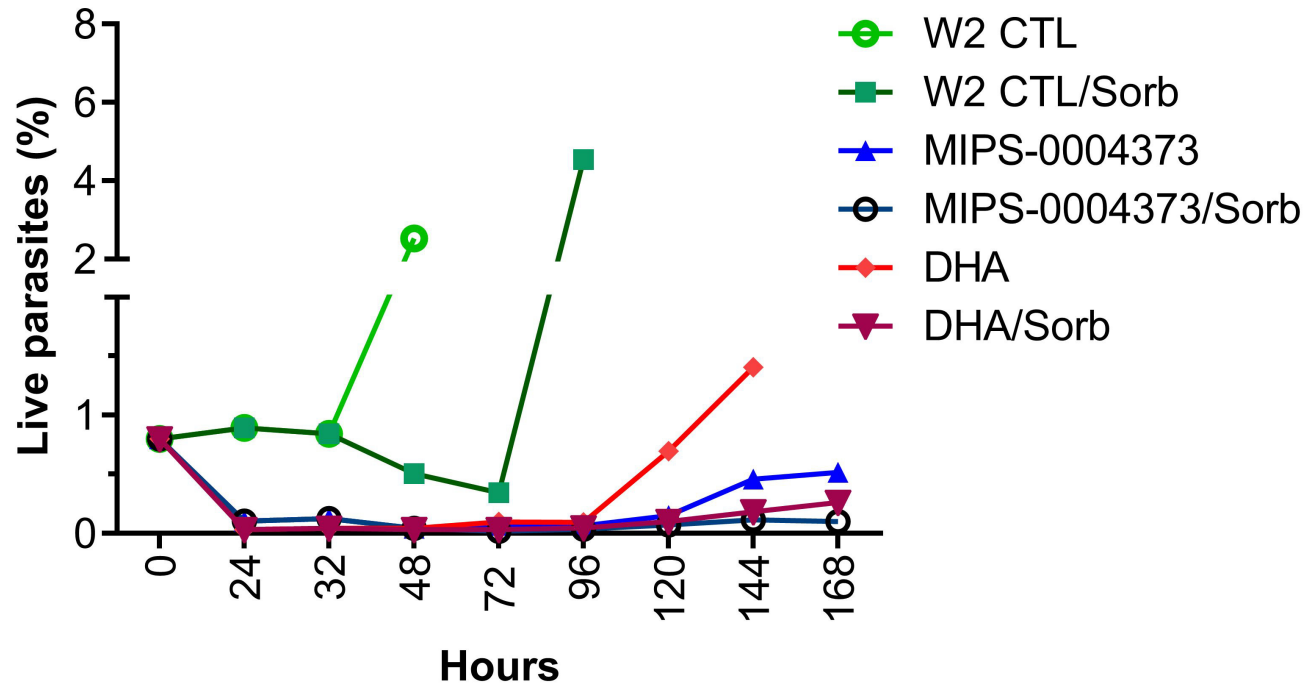
1019 **Figure 6:** *In vitro* chemoprotective effect of MIPS-0004373 against liver stage parasites. **A.**
1020 Freshly dissected *P. berghei* sporozoites expressing luciferase were dispensed onto HepG2
1021 hepatocytes pretreated with increasing concentrations of MIPS-0004373. Activity was
1022 determined from the bioluminescence of viable parasites after a 48 h incubation, during
1023 which MIPS-0004373 (black circle) acted in a dose dependent manner. Average survival (%)
1024 of extra-erythrocytic forms (EEFs) is shown against atovaquone (1 μ M; purple dashed line)
1025 and DMSO (0.5%; blue dashed line). **B.** Uninfected HepG2 hepatocytes showed
1026 susceptibility to MIPS-0004373 (black circle) at ≥ 5.55 μ M, but remain largely insensitive at
1027 concentrations relevant to antimalarial effect. Average HepG2 survival (%) is shown with
1028 puromycin (5 μ M; green dashed line) and DMSO (0.5%; blue dashed line). These data
1029 represent three biological replicates against *P. berghei* liver stages and four biological
1030 replicates in the HepG2 cytotoxicity evaluation (error bars = SEM). **C.** Three point 10-fold
1031 dilution series (0.1, 1, and 10 μ M) for MIPS-0004373 activity against *P. cynomolgi* liver
1032 stage cultures. The percentage of untreated control is shown as a function of test compound
1033 concentration. Differential counting of schizonts and hypnozoite forms was performed based
1034 on size and number of parasite nuclei. The results of three assays are shown. KAI407 is
1035 included as a positive control known to have a liver stage activity profile similar to that of
1036 primaquine (24), and the untreated samples are vehicle controls (DMSO). Small liver stage
1037 forms are represented by the dark bars and large forms by the light bars.

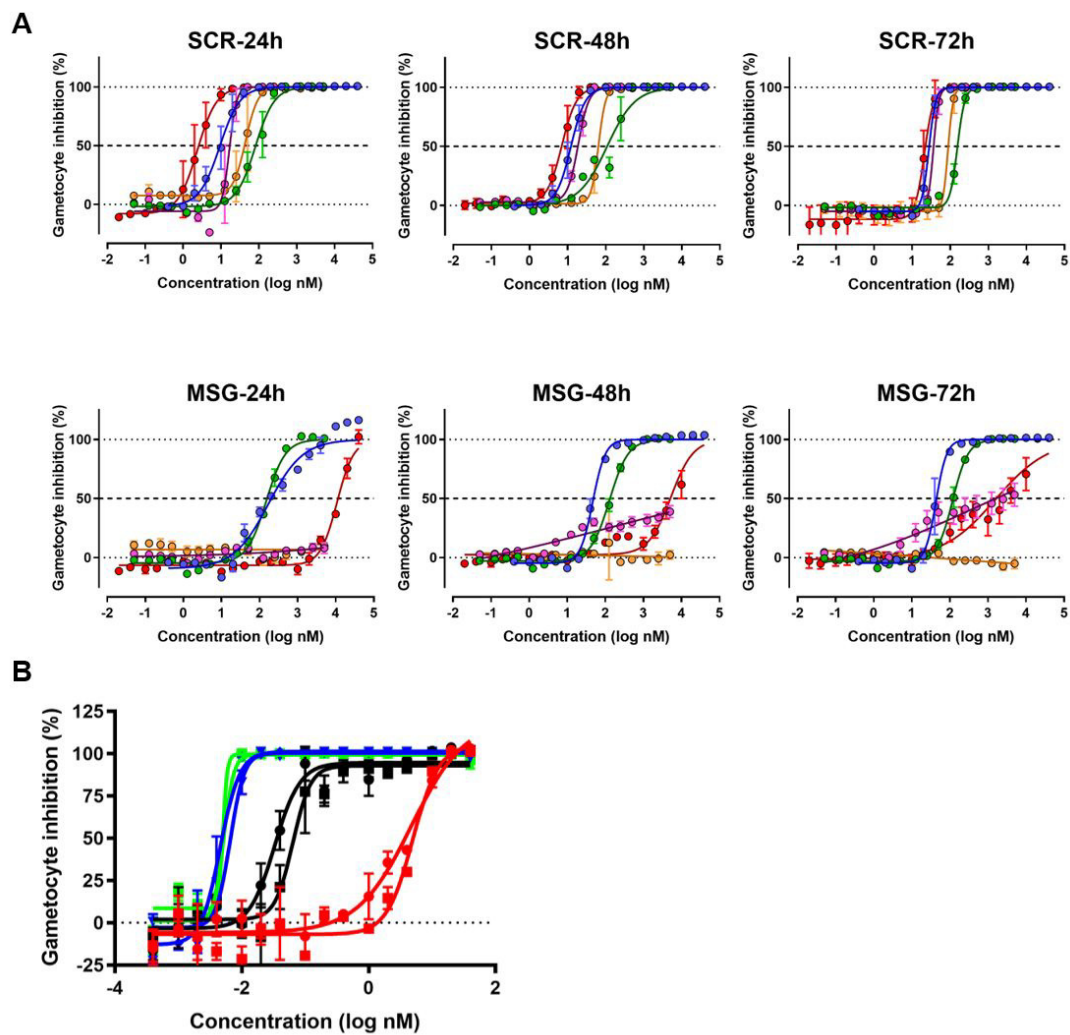
1038

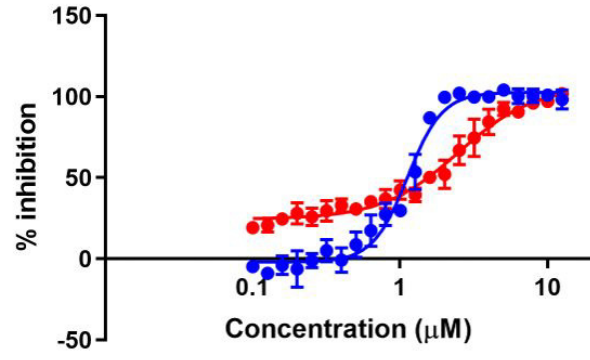
1039









A**B**